Global Change Biology (2005) **11,** 1118–1130, doi: 10.1111/j.1365-2486.2005.00974.x

Spatial and temporal variation of phenological growing season and climate change impacts in temperate eastern China

XIAOQIU CHEN, BING HU and RONG YU

Department of Geography, College of Environmental Sciences, MOE Laboratory for Earth Surface Processes, Peking University, Beijing 100871, China

Abstract

Using phenological and normalized difference vegetation index (NDVI) data from 1982 to 1993 at seven sample stations in temperate eastern China, we calculated the cumulative frequency of leaf unfolding and leaf coloration dates for deciduous species every 5 days throughout the study period. Then, we determined the growing season beginning and end dates by computing times when 50% of the species had undergone leaf unfolding and leaf coloration for each station year. Next, we used these beginning and end dates of the growing season as time markers to determine corresponding threshold NDVI values on NDVI curves for the pixels overlaying phenological stations. Based on a cluster analysis, we determined extrapolation areas for each phenological station in every year, and then implemented the spatial extrapolation of growing season parameters from the seven sample stations to all possible meteorological stations in the study area.

Results show that spatial patterns of growing season beginning and end dates correlate significantly with spatial patterns of mean air temperatures in spring and autumn, respectively. Contrasting with results from similar studies in Europe and North America, our study suggests that there is a significant delay in leaf coloration dates, along with a less pronounced advance of leaf unfolding dates in different latitudinal zones and the whole area from 1982 to 1993. The growing season has been extended by 1.4–3.6 days per year in the northern zones and by 1.4 days per year across the entire study area on average. The apparent delay in growing season end dates is associated with regional cooling from late spring to summer, while the insignificant advancement in beginning dates corresponds to inconsistent temperature trend changes from late winter to spring. On an interannual basis, growing season beginning and end dates correlate negatively with mean air temperatures from February to April and from May to June, respectively.

Keywords: air temperature, climate change, interannual variability, linear trend, normalized difference vegetation index, phenological growing season, spatial extrapolation, spatial pattern, temperate eastern China

Received 3 April 2004; revised version received 18 October 2004; accepted 23 February 2005

Introduction

Detecting growing season variability of terrestrial vegetation is crucial for identifying responses of ecosystems to recent climate change at seasonal and interannual time scales (Chen *et al*., 2001; Walther *et al*., 2002). A lengthening of the growing season in northern vegetation over the past decades is speculated based on observed changes in the seasonal signal in atmospheric CO_2 (Keeling *et al*., 1996) and satellite observations (Myneni *et al*., 1997; Zhou *et al*., 2001). These atmospheric and satellite data are supported by field-based phenological observation of plants (Ahas, 1999; Bradley *et al*., 1999; Menzel & Fabian, 1999; Beaubien & Freeland, 2000; Chmielewski & Roetzer, 2001; Fitter & Fitter, 2002) and simulations from a dynamic vegetation model (Lucht *et al*., 2002), especially the significant

Correspondence: Xiaoqiu Chen, tel. + 86 10 62875174, fax + 86 10 62751187, e-mail: cxq@pku.edu.cn

advancement of phenological events in spring and the less pronounced delay of phenological events in autumn across Europe and North America. Recent global meta-analyses strongly suggest that these phenological fingerprints implicate climate change as an important driving force on natural systems (Parmesan & Yohe, 2003; Root *et al*., 2003).

In China, however, phenological stations and conventional phenological data are comparatively scarce; therefore, the options for detecting growing season trends are to estimate the growing season of land vegetation using limited station phenological and climate data, or with satellite data (Chen & Pan, 2002). In the former case, a simple phenological model, driven by daily maximum–minimum temperatures can be employed as a surrogate measure of the onset of spring. Contrasting with the result from a similar study in North America (Schwartz & Reiter, 2000), the onset of spring plant growth derived from modelled lilac first leaf and first bloom dates in China showed no apparent linear trend from 1959 to 1993 (Schwartz & Chen, 2002). In the latter case, various methods have been developed to determine a satellite-sensor-derived growing season at different spatial scales using the normalized difference vegetation index (NDVI) data derived from the advanced very high-resolution radiometer (AVHRR) or the enhanced vegetation index data derived from the moderate-resolution imaging spectroradiometer (Lloyd, 1990; Fisher, 1994; Reed *et al*., 1994; Markon *et al*., 1995; Moulin *et al*., 1997; White *et al*., 1997; Botta *et al*., 2000; Zhang *et al*., 2004). However, because metrics and thresholds of vegetation indices may not directly correspond to conventional, ground-based phenological events, but rather provide indicators of vegetation dynamics (Reed *et al*., 1994), a detailed comparison of these satellite measures with ground-based phenological events is needed (Schwartz, 1998; Chen *et al*., 2000). In recent years, some studies have been carried out to compare satellite-sensor-derived onset and offset of greenness with surface phenological stages of individual plant species, mono-specific forests, and mixed forests for selected biomes (White *et al*., 1997; Duchemin *et al*., 1999; Schwartz *et al*., 2002; Badeck *et al*., 2004). Other than the above top-down method, namely determining the satellite-sensor-derived growing season at a regional scale first, and then validating it using conventional phenological data at local scales, Chen *et al*. (2000, 2001) developed a bottom-up method, namely determining the phenological growing season at sample stations first and then finding out the corresponding threshold NDVI values at pixels overlaying the sample stations in order to extrapolate the phenological growing season at a regional scale. To implement the above goal, the objectives of this study were to (1) extrapolate the phenological growing season of plant community in temperate eastern China, using threshold NDVI values obtained by phenology-satellite analyses at sample stations, (2) identify spatial patterns and trends of growing season parameters (beginning, end, and length) at local, zonal, and regional scales; and (3) assess the relationship between growing season parameters and seasonal air temperatures with respect to spatial and temporal variations.

Materials and methods

Study area

Situated in the southeastern part of the Eurasian Continent on the west coast of the Pacific Ocean, China is world famous for its monsoonal climate caused by the difference in heat reserves between the world's largest continent and the world's biggest ocean. Monsoonal winds bring the most striking seasonal changes to the vast eastern areas of China, especially in the temperate zone, which is cold and dry in winter and warm and humid in summer. Because seasonal biome dynamics are controlled by recurrent variations of environmental conditions, especially climate, seasonal biome features in temperate areas with distinct climatic rhythmicity are rich and colorful (Chen, 2003a). Therefore, we selected a study area that is located from 32°N to the northern border (53°31′N) of China and from 106°E to the eastern border (135°03′E) or the coastline of China. The parallel 32°N and the meridian 106°E represent approximately the southern border of the temperate zone in eastern China (Zhang & Lin, 1985) and the west edge of the influence of the summer monsoon, respectively (Gao *et al*., 1962). The study area covers the cold temperate, middle temperate, and warm temperate zones. The dominant vegetation types include conifer forest in the cold temperate zone, deciduous broad-leaved and coniferous mixed forest and steppe in the middle temperate zone, deciduous broad-leaved forest in the warm temperate zone, and various interzonal crops (Compilation Committee on the Vegetation of China, 1980). In order to determine the ground-based growing season and assess the relationship between growing season parameters and climate factors, we selected seven phenological stations and 125 meteorological stations altogether as sample sites (Fig. 1). The selection of the seven phenological stations, namely Harbin (45°45′N, 126°40′E, 146 m), Mudanjiang (44°26′N, 129°40′E, 300 m), Gaixian (40°26′N, 122°20′E, 45 m), Beijing (40°01′N, 116°20′E, 50 m), Xingtai (37°04′N, 114°30′E, 77 m), Luoyang (34°40′N, 112°25′E, 155 m), and Xi'an (34°13′N, 108°58′E, 438 m), was based on diversity of the plant

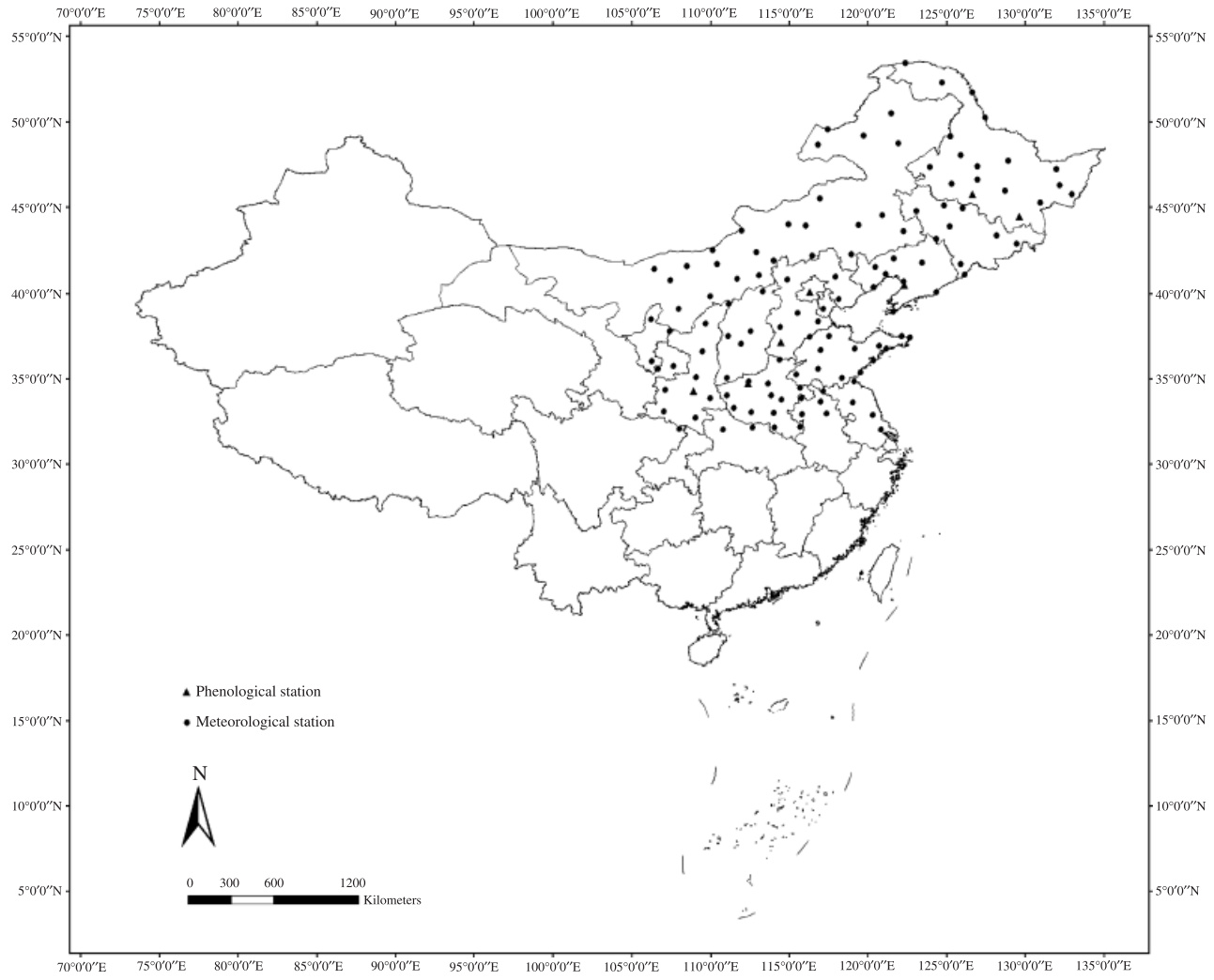

Fig. 1 Location of phenological and meteorological stations.

species (>30) and accuracy of the observations. As there are parallel phenological and meteorological observations at Harbin, Mudanjiang, Beijing, Xingtai, and Xi'an, the total number of individual sample stations is 127. Most of the phenological and meteorological stations are located within suburbs of cities with less significant urban heat island effects.

Phenology and climate data

Because phenological observation and study have important applications in directing agricultural production, the Chinese Academy of Sciences (CAS) established a countrywide phenological network in the early 1960s. Observations began in 1963 and continued until 1996. In 2003, phenological observations were resumed. The observation program of the CAS network included a total of 173 observed species. Of these, 33 species of woody plants, two species of herbaceous plants, and 11 species of fauna were observed across the network (Chen, 2003b). The observed trees and shrubs were selected according to spatial comparability and local representativeness and the observations were carried out mainly by botanical gardens, research institutes, and universities according to uniform observation criteria (Institute of Geography at Chinese Academy of Sciences, 1965). The phenophases of woody plants included bud burst, first leaf unfolding, 50% leaf unfolding, flower bud or inflorescence appearance, first bloom, 50% bloom, end of blooming, fruit or seed maturing, fruit or seed shedding, first leaf coloration, full leaf coloration, first defoliation, and end of defoliation. Phenological data used in this study were acquired from Chinese Yearbooks of Animal and Plant Phenological Observation for the period of 1982–1988 compiled by the Institute of Geography at Chinese

Academy of Sciences (1988, 1989a, b, 1992) and from an unpublished data set for the period of 1989–1993 provided by the Institute of Geography at CAS. The study period ends in 1993 because the data in the last 3 years (1994–1996) were not available. In order to conduct joint analyses of plant phenology and satellite data, we chose leaf unfolding and leaf coloration as indicator events to show the start and end of the growing season of local plant communities. The data of leaf unfolding and leaf coloration of all observed deciduous trees and shrubs at the sample sites were verified and revised according to the inherent sequence of occurrence dates of phenophases and the linear correlation between time series of phenophases at each site (Yang & Chen, 1995).

As the occurrence dates of phenological events of the observed woody plants correlated closely with those of forest trees, herbs, and crops (Schnelle, 1955; Brandtner, 1958; Chu, 1964; Pfau, 1964), and served as a measure of equal physiological development correlated with current and accumulative climatic factors (Newman & Beard, 1962; Chu, 1964), the observed trees and shrubs were usually applied as indicator species to deduce the development of forest trees, herbs, and crops, and to determine the correct time for forest and farm tasks (Hopkins & Murray, 1933; Chu & Wan, 1973). Extending this approach, we can also use the observed plants and phenophases of the CAS network as indicator species and indicator events to represent the local plant community and its seasonality in temperate eastern China.

It is well known that air temperature is the most important controlling factor related to trees' phenology in the temperate zone (Romberger, 1963; Chen, 1994; Kramer, 1996; Chmielewski & Roetzer, 2001; Zhang *et al*., 2004), whereas precipitation and photoperiod play a less pronounced role in phenological development (Chen, 1994; Chen & Pan, 2002). Dealing with the selection of temperature parameters, the heat unit, expressed in growing degree days (GDD) is frequently used to describe the timing of phenological stages and simulate the phenological development of woody plants (McMaster & Wilhelm, 1997; Murray *et al*., 1989; Haenninen, 1990; Kramer, 1996), while monthly and seasonal mean temperatures are usually applied to analyze statistical relationships between plant phenology and climate conditions (Beaubien & Freeland, 2000; Sparks *et al*., 2000; Chmielewski & Roetzer, 2001; Chen & Pan, 2002; Fitter & Fitter, 2002; Menzel, 2003). In the present study, daily mean air temperatures at the 125 meteorological stations from January 1982 to December 1993 were processed into monthly and annual mean air temperatures for each station, which then served as the driving parameter for carrying out a correlation analysis between the beginning and end dates of the growing season and mean air temperatures prior to and during the beginning and end dates.

Satellite data

Satellite data were derived from the AVHRR on the 'afternoon' NOAA operational meteorological satellite. The NDVI was obtained from the NOAA/NASA Pathfinder AVHRR Land data set for 1982–1993 at 8 km spatial resolution. The NDVI composites were generated by selecting the highest NDVI value over each 10-day period in order to reduce the effect of cloud contamination. Using Geographic Information Systems software (ArcInfo), we produced an NDVI data set corresponding to pixels overlaying the phenological and meteorological stations during 1982–1993. Because of the inherent nature in AVHRR data acquisition and processing because of satellite viewing geometry (Goward *et al*., 1991), atmospheric haze and cloud, and temporal data composites (Holben, 1986), the 10-day NDVI composites can be biased. These effects result in reduced NDVI values. To compensate for the effects, we used a smoothing method suggested by Chen *et al*. (2000) to modify the maximum value composite NDVI data at pixels overlaying the sample stations. For the NDVI value of every 'nth' 10-day period within a year, we calculated the mean value of the $(n-1)$th and $(n+1)$th 10-day periods and then compared this mean with the value for the original nth 10-day period. If the mean value was greater than the original value, we replaced the original with the mean as the NDVI value of the nth 10-day period; if the mean NDVI value was smaller than the original NDVI value, we retained the original. As the maximum value composite technique has eliminated some high-frequency 'noises' in the NDVI profiles, the smoothing method we proposed would probably be better appropriate for reducing residual 'noises' than methods for extracting NDVI profiles from daily data (e.g. the best index slope extraction) (Viovy *et al*., 1992).

Determining the growing season and threshold NDVI values at sample sites

Many studies have shown that NDVI is sensitive to variations in vegetation coverage or density and provides an efficient tool to document the biophysical state of the continental surfaces (Justice *et al*., 1985; Malingreau, 1986; Viovy & Saint, 1994; Moulin *et al*., 1997; White *et al*., 1997; Botta *et al*., 2000). Among the surface parameters that can be related to satellite sensor-derived greenness development, plant phenology is a key measure related to seasonal vegetation

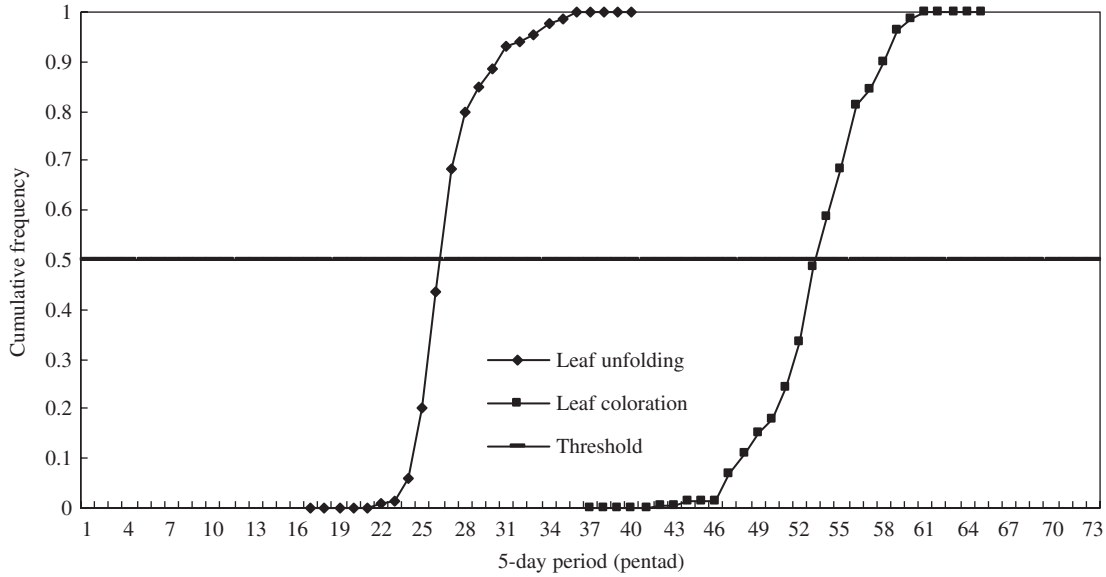

Fig. 2 Determining growing season beginning and end dates at a phenological station.

coverage and density in the temperate zone (Viovy & Saint, 1994; Chen & Pan, 2002). As NDVI measurements integrate observations of different plants and tend to provide descriptive characteristics of phenological landscape events, rather than direct associations with the phenological performance of specific plants during the growing season (Achard & Blasco, 1990; Reed *et al*., 1994), phenological data of local plant communities are more suitable for surface satellite analyses than those of individual plant species. Previous comparisons between temporal NDVI profiles and frequency curves of occurrence dates of all plant phenophases at the biome level show that they have similar patterns in spring and autumn (Chen *et al*., 2001). This relationship validates that the NDVI curve represents 'green wave' development in spring and 'brown wave' development in autumn. For this current study, we have redefined the growing season as the time interval between the date on which 50% of all observed trees and shrubs enter leaf unfolding in spring and the date on which 50% of all observed trees and shrubs enter leaf coloration in autumn. Thus, the growing season will approximate the photosynthetic period of vegetation, and in turn, should have a closer link with satellite-sensor-derived greenness development than its early forms.

First, we calculated the case, frequency, and cumulative frequency of leaf unfolding and leaf coloration of all plants within every 5-day period throughout each year (from January 1 to December 31) at each phenological station, and then drew the cumulative frequency curves of leaf unfolding and leaf coloration, respectively. Next, we determined growing season beginning and end dates on the cumulative frequency curve by computing interpolation dates when the cumulative frequency of leaf unfolding and leaf coloration reaches 50% for each station and each year (Fig. 2). As the phenological data at Harbin in 1992 and 1993 and at Xi'an in 1992 were missing, we estimated the growing season beginning and end dates for both stations and the above years using a spatial interpolation technique (Yang & Chen, 1995). The reliability of interpolation can be partially documented by spatial sequences of growing season beginning and end dates at sample sites in the corresponding years (not showed). Moreover, we used growing season beginning and end dates as time markers to determine the corresponding threshold NDVI values on the NDVI curves at pixels overlaying phenological stations from year to year (Fig. 3). Table 1 shows that beginning of the growing season is earlier at southern stations and later at northern stations, but end of the growing season is earlier at northern stations and later at southern stations. Generally, the threshold NDVI values at the beginning of the growing season in the south are larger than in the north, whereas the threshold NDVI values at the end of the growing season in the north are larger than in the south.

Statistical extrapolations of the growing season in temperate eastern China

To extrapolate the growing season beginning and end dates to meteorological stations using threshold NDVI values obtained at the seven phenological stations, the spatial extrapolation area of each phenological station

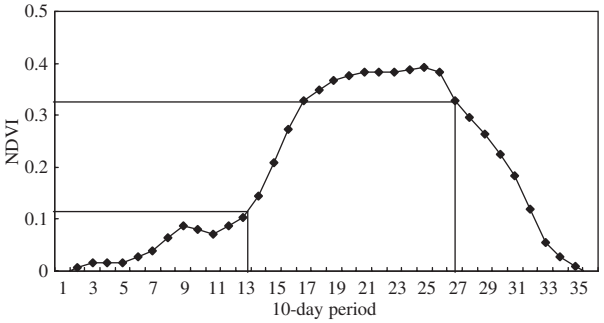

Fig. 3 Determining corresponding threshold NDVI values at a phenological station.

Table 1 Mean (day of year) and standard deviation (days) of BGS and EGS and corresponding threshold normalized difference vegetation index (NDVI) values at phenological stations from 1982 to 1993

Station	Parameter	BGS	NDVI at BGS	EGS	NDVI at EGS
Harbin	Mean	127	0.171	269	0.370
	SD	5	0.031	5	0.042
Mudanjiang	Mean	124	0.381	268	0.612
	SD	5	0.101	3	0.044
Gaixian	Mean	112	0.153	287	0.341
	SD	5	0.026	13	0.103
Beijing	Mean	105	0.175	298	0.256
	SD	5	0.066	5	0.057
Xingtai	Mean	103	0.334	292	0.258
	SD	7	0.081	7	0.033
Luoyang	Mean	100	0.433	295	0.289
	SD	3	0.109	6	0.066
Xi'an	Mean	98	0.447	299	0.278
	SD	4	0.093	5	0.089

BGS, beginning of the growing season; EGS, end of the growing season.

was identified. As one of the preconditions for spatial extrapolation is that the annual NDVI curves at the pixels overlaying the extrapolation sites should be coincident with that at the pixel overlaying a phenological station (Chen *et al.*, 2001), a spatial extrapolation area can be determined by comparing the coincidence of the NDVI curves among the corresponding pixels. For this study, the NDVI data matrix consisted of 127 rows (representing stations/pixels) and 36 columns (representing 10-day periods). We measured the coincidence of the NDVI curves using the Euclidean distance (d_{ik}):

$$d_{ik} = \sqrt{\sum_{j=1}^{36} (x_{ij} - x_{kj})^2},$$

where x_{ij} and x_{kj} are the 10-day peak NDVI values at the ith pixel and the kth pixel, and j is the ordinal number of the 10-day periods in a year. We carried out a hierarchical cluster analysis to define extrapolation areas for phenological stations in each year. Considering the appropriate number of final clusters and the significant difference of d_{ik} values between clustering stages, we assigned the maximum d_{ik} for determining the final clusters between 0.52 and 0.78 during 1982–1993. Generally, the smaller the maximum d_{ik} of a cluster in a given year, the higher the coincidence of NDVI curves of the pixels within the cluster. As a result, the number of extrapolation areas changes between 4 and 7. Here, we assume that the threshold NDVI values indicating the growing season beginning and end at the extrapolation sites are the same as those at the phenological station within an extrapolation area and in a given year. Therefore, we can directly estimate the growing season beginning and end dates at the extrapolation sites on their NDVI curves from 1982 to 1993 using the yearly threshold NDVI values at the phenological stations. In order to decrease the bias, the precise beginning and end dates were set at the center of the 10-day periods, namely the sixth day. The time series of growing season parameters at the seven phenological stations and the 82 extrapolation sites (Fig. 4) with more than 8 years of data provide the basis for further analyses.

To detect the growing season variability in response to climate change, we carried out two types of analyses: spatial pattern analysis and temporal trend analysis. For the former analysis, we revealed the spatial relationship between average growing season parameters (beginning and end date) and mean air temperatures at the sites over the 1982–1993 period. For the latter analysis, because the importance of nonclimatic mechanisms determining growing season changes should decrease with increasing scale (Parmesan & Yohe, 2003), we focused on the trend analysis at both zonal and regional scales. First, we divided the research region into five latitudinal zones: 32–34.99°N (zone 1), 35–37.99°N (zone 2), 38–40.99°N (zone 3), 41–43.99°N (zone 4), and $\geq$ 44°N (zone 5). Secondly, we used the station time series to create the average zonal and regional time series. Lastly, we calculated simple linear trends for these time series and tested their significance using Pearson's correlation coefficients and *t*-tests.

Results and discussion

Spatial relationship between growing season and air temperature

Generally, average beginning dates of the local growing season progress from south to north and from coastal

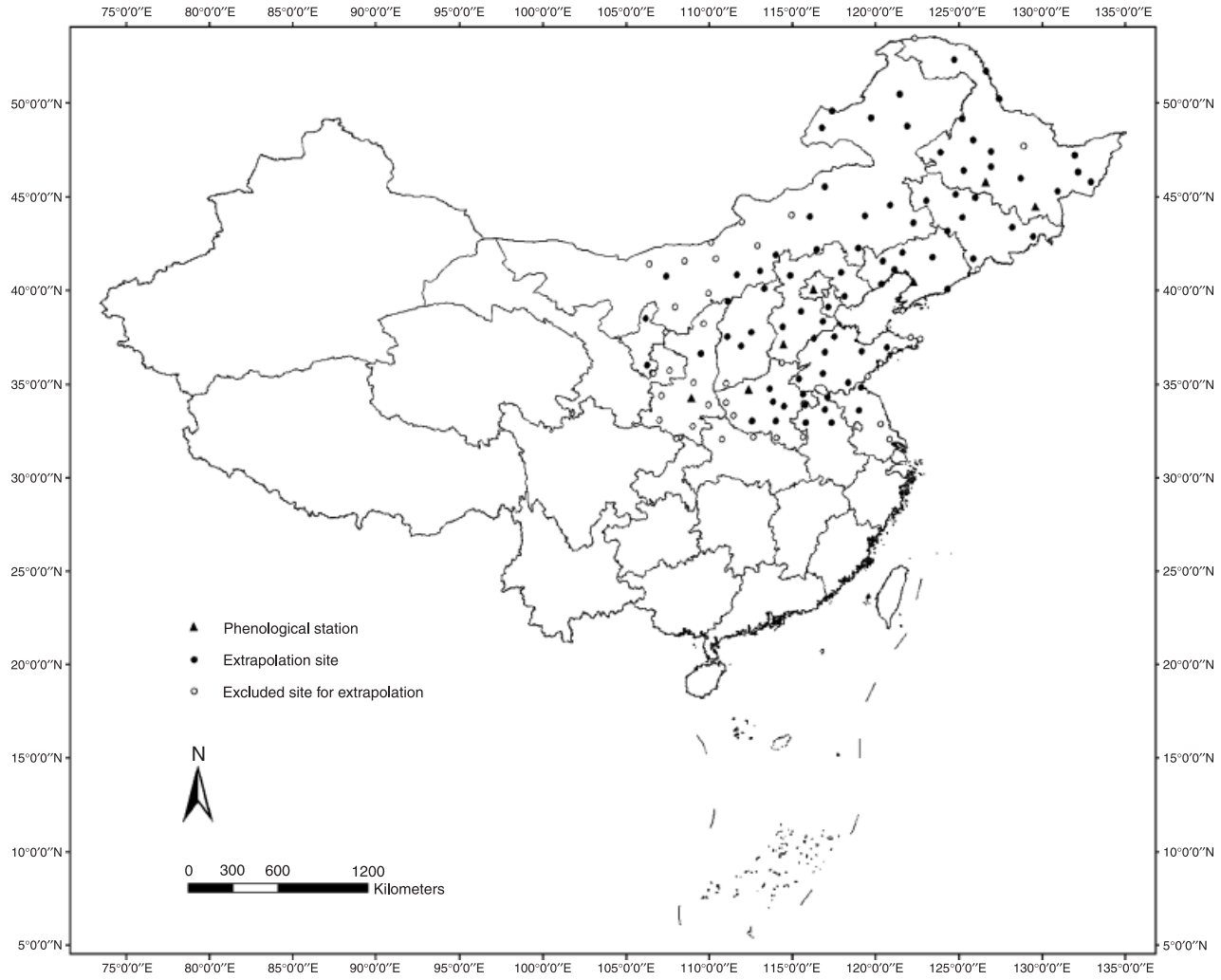

Fig. 4 Location of phenological stations and extrapolation sites and excluded sites for extrapolation.

areas (lower altitudes) to inland areas (higher altitudes). In contrast, average end dates of the local growing season progress roughly from north to south and from inland areas (higher altitudes) to coastal areas (lower altitudes). Local heat and energy regimes are the cause of this spatial progression pattern.

A spatial correlation and regression analysis between average growing season parameters and mean air temperatures prior to and during the beginning and end dates of the growing season at all sites shows that beginning date of the growing season correlates closely with mean temperature from March to May ($R^2 = 0.6966$, $n = 87$, $P < 0.001$). The multinomial simulation (Fig. 5) shows that the dependence of beginning of the growing season on mean temperature is much stronger at sites with March–May temperature above 8 °C (linear correlation coefficient $r = -0.8276$, $n = 51$, $P < 0.001$) than at sites with March–May temperature below 8 °C (linear correlation coefficient $r = -0.0454$, $n = 36$, $P > 0.1$). The negative correlation indicates that the higher the mean temperature during March and May at a site, the earlier the average growing season beginning time. In contrast, there is a highly linear correlation between end date of the growing season and mean temperature from August to October ($r = 0.8204$, $n = 87$, $P < 0.001$). The positive correlation indicates that the higher the mean temperature during August and October at a site, the later the average growing season end time (Fig. 6).

Growing season trends and interannual variability

An advance of 0.7–1.7 days per year in growing season beginning dates is detectable from zones 2 to 5 with a relatively low significance level (Fig. 7a), whereas a delay in end dates occurred in all five zones and a

significant delay of 0.9–1.9 days per year appeared in zones 2–4 (Fig. 7b). The growing season duration was, therefore, significantly lengthened by 1.4–3.6 days per year from zones 2 to 5 (Fig. 7c). A reversed trend in beginning dates and a slightly consistent trend in end dates were observed in zone 1. The stronger linear trends in all higher latitudinal zones indicate that the growing season has a widespread and concordant pattern of change.

However, the northernmost zone did not show larger linear trends towards advanced spring events or delayed autumn events than southern zones did as global meta-analyses suggest (Root *et al.*, 2003). The attribution of the weakened trends in zone 5 is complicated because physiological and environmental factors dominate local phenological changes. Possible

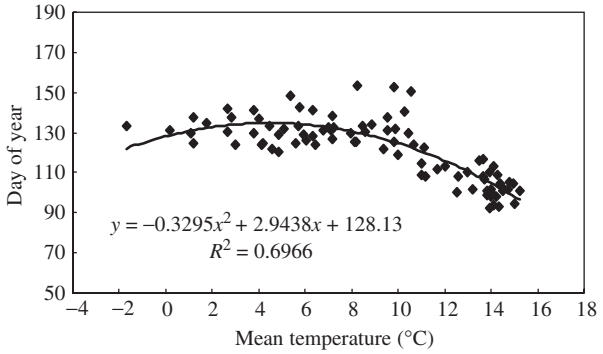

Fig. 5 Spatial relationships between March–May mean temperatures and average growing season beginning dates from 1982 to 1993.

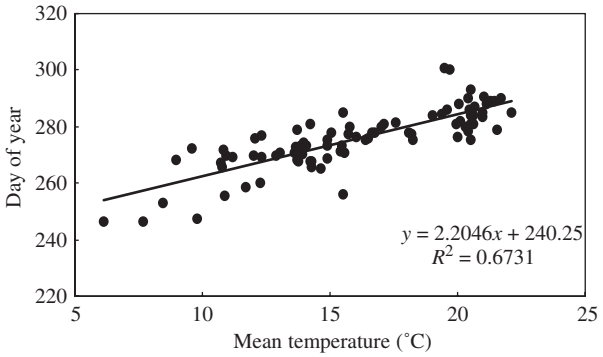

Fig. 6 Spatial relationships between August–October mean temperatures and average growing season end dates from 1982 to 1993.

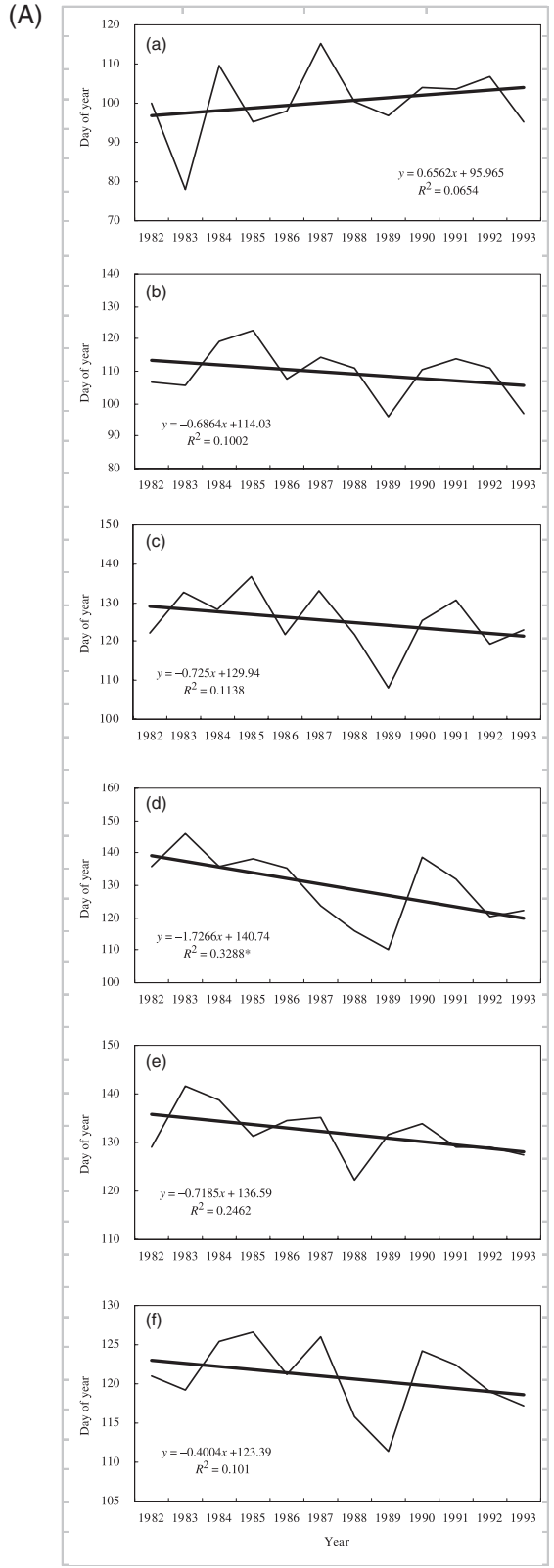

Fig. 7 (A) Linear trends of growing season beginning date. (a) zone 1; (b) zone 2; (c) zone 3; (d) zone 4; (e) zone 5; (f) whole area; $*P<0.1$. (B) Linear trends of growing season end date. (a) zone 1; (b) zone 2; (c) zone 3; (d) zone 4; (e) zone 5; (f) whole area; $**P<0.05$; $***P<0.01$; $****P<0.001$. (C) Linear trends of growing season length. (a) zone 1; (b) zone 2; (c) zone 3; (d) zone 4; (e) zone 5; (f) whole area; $**P<0.05$; $***P<0.01$.

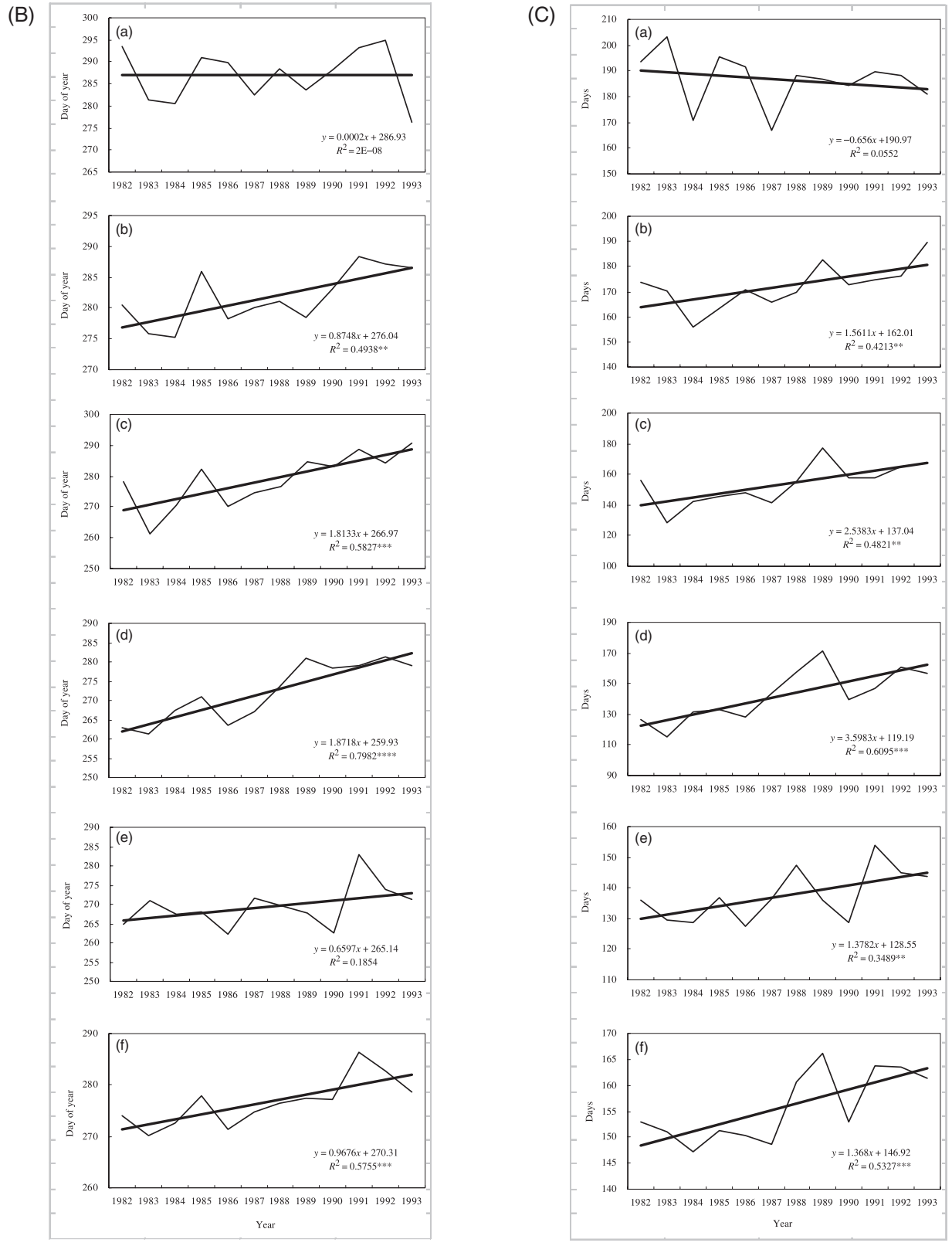

Fig. 7 (*Continued*)

Table 2 Linear trends (°C/year) of monthly and seasonal and annual mean temperatures in different zones and for the whole area from 1982 to 1993

Period	Zone 1	Zone 2	Zone 3	Zone 4	Zone 5	Area
December	+0.10	+0.15	+0.14	+0.11	+0.04	+0.11
January	−0.01	+0.04	+0.09	+0.14	+0.11	+0.07
February	+0.22†	+0.38	+0.26†	+0.32†	+0.35†	+0.31†
Winter	+0.10	+0.19	+0.17	+0.19	+0.17	+0.16
March	−0.02	+0.04	+0.14	+0.21	+0.32	+0.14
April	+0.01	−0.03	−0.04	−0.10	−0.06	−0.04
May	−0.18†	−0.14†	−0.06	−0.01	+0.05	−0.07*
Spring	−0.06	−0.04	+0.01	+0.03	+0.10	+0.01
June	+0.01	−0.02	−0.04	−0.11†	−0.07	−0.05
July	+0.13	+0.04	+0.01	−0.02	+0.01	+0.03
August	−0.08	−0.04	+0.01	−0.03	−0.05	−0.04
Summer	+0.02	−0.00	−0.01	−0.05	−0.04	−0.02
September	+0.10	+0.11	+0.05	+0.03	+0.00	+0.06
October	−0.04	−0.09	−0.08	−0.00	+0.25†	+0.01
November	−0.10	−0.08	−0.07	−0.04	+0.03	−0.05
Autumn	−0.01	−0.02	−0.03	−0.01	+0.09	+0.00
Year	+0.01	+0.02	+0.03	+0.04	+0.08	+0.04

*$P<0.1$, †$P<0.05$.

ecological explanations for the reduced trend of growing season beginning dates in the highest latitudinal zone are regional warming in winter (Table 2) and physiological response of plants to the regional warming. As certain cultivars show, woody plants have higher chilling requirements for resuming growth after winter dormancy in cold climates relative to warm climates (Powell, 1986). If chilling cannot be completely satisfied because of significantly increasing temperatures during the dormancy period, then more heat units (GDD) are required for the onset of plant growth in spring (Couvillon & Erez, 1985; Cannell & Smith, 1986; Powell *et al*., 1986; Murray *et al*., 1989), which could slow the advancement of spring phenophases in the highest latitudinal zone under a less pronounced temperature increase in spring (Table 2).

Linear trends were also observed at the regional scale: growing season beginning date advanced by 0.4 days per year with low significance (Fig. 7a), whereas end date was significantly delayed by 1 day per year and length was significantly extended by 1.4 days per year (Fig. 7b and c). The significant extension of growing season duration by 1.4 days per year for our ground-based time series (1982–1993) is consistent with time series of satellite observations in the northern high latitudes (1981–1991, 12 days per decade, Myneni *et al*., 1997) and in Eurasia (1981–1999, 10 days per decade, Zhou *et al*., 2001). The trend in growing season beginning date in temperate eastern China is also consistent with the trend in growing season beginning date in Europe (Chmielewski & Roetzer, 2001), but is not as strong as the trend of first-leaf spring index date in eastern North America over roughly the same period (1980–1990, 9 days per decade, Schwartz, 1998). In contrast, the trend in growing season end date in temperate eastern China is much stronger than that in Europe (Chmielewski & Roetzer, 2001).

In terms of interannual variability, the earliest growing season beginning date appeared in the end of 1980s (1988 or 1989), whereas the latest end date occurred in the beginning of 1990s (1991 or 1992) in most zones and the whole area (Fig. 7a and b). A significant correlation in growing season duration exists between adjacent zones, such as, between zones 2 and 3 (Pearson's correlation $r=0.754$, $P<0.01$), between zones 3 and 4 ($r=0.839$, $P<0.001$), and between zones 4 and 5 ($r=0.589$, $P<0.05$). However, the spatial similarity of time series of growing season duration decreases rapidly as the distance between latitudinal zones increases in temperate eastern China (not shown).

Temporal relationship between growing season and air temperature

The growing season extension we detect in this study corresponds with an increasing trend in annual mean temperature in northeast China from 1951 to 1994 (Wang & Gaffen, 2001), and in different latitudinal zones and whole study area from 1982 to 1993 (Table 2). Examination of monthly mean temperatures shows a warming from December to March and in July and

Table 3 Correlation coefficients (r) between growing season parameters and mean air temperatures in different zones and for the whole area from 1982 to 1993

Correlation variables	$r_{(\text{zone 1})}$	$r_{(\text{zone 2})}$	$r_{(\text{zone 3})}$	$r_{(\text{zone 4})}$	$r_{(\text{zone 5})}$	$r_{(\text{area})}$
BGS-T_2	+0.07	$-0.64^{\dagger}$	−0.47	−0.45	−0.33	−0.44
BGS-T_3	−0.21	$-0.71^{\ddagger}$	−0.54*	+0.00	+0.02	−0.39
BGS-T_4	−0.47	−0.18	−0.47	−0.12	−0.26	−0.48
BGS-$T_{2–4}$	−0.28	$-0.78^{\ddagger}$	$-0.63^{\dagger}$	−0.24	−0.19	−0.54*
EGS-T_5	+0.30	$-0.58^{\dagger}$	−0.44	−0.03	−0.00	$-0.60^{\dagger}$
EGS-T_6	+0.12	+0.01	−0.42	$-0.63^{\dagger}$	−0.34	−0.34
EGS-$T_{5,6}$	+0.30	−0.50*	−0.53*	−0.50*	−0.32	$-0.61^{\dagger}$

T_2, T_3, T_4, and $T_{2–4}$, mean air temperatures in February, March, April, and from February to April.
T_5, T_6, and $T_{5,6}$, mean air temperatures in May, June, and from May to June.
*$P<0.1$, $^{\dagger}P<0.05$, $^{\ddagger}P<0.01$.

September, with the most significant temperature increase in February, and cooling from April to June and in August and November in most zones and the entire study area (Table 2). The unsteady changes of temperature trends from February to April may result in the slight advancement of growing season beginning dates, whereas the dominant cooling from May to August may cause the apparent delay of end dates. Just as buds have a required heat accumulation for flushing, leaf life and senescence are also mediated by heat accumulation (Worrall, 1998). A later end of the growing season, as judged by later leaf coloration dates, would have been because of the leaves' heat sum not being met as early as in previous years, because of cool summer temperatures, rather than a mild autumn (Worrall, 1999). Nevertheless, more detailed studies and explanations are needed to understand the physiological and ecological mechanisms of this relationship.

On an interannual basis, correlation analysis shows that growing season beginning dates were mainly influenced by mean air temperatures from February to April, especially in zones 2 and 3 and the whole area (Table 3). A negative correlation indicates that higher mean temperatures in late winter and spring trigger an earlier onset of the growing seasons of local plant communities. In contrast to beginning dates, a significant correlation between growing season end dates and mean air temperatures from May to June was detectable from zones 2 to 4, as well as across the entire study area (Table 3). The overall negative correlation indicates that lower mean temperatures during late spring and early summer induce a later end of the growing season. A similar result was also reported in Germany (Menzel, 2003).

Conclusions

The current study has employed spatial extrapolation of growing season parameters from several sample sites to an area. Spatial patterns of the growing season beginning and end dates correlate significantly with spatial patterns of mean air temperatures in spring and autumn, respectively. Contrasting with results from similar studies in Europe and North America, our study suggests that (1) the growing season and the photosynthetic period of land vegetation in temperate eastern China has significantly extended during a shorter period of time, (2) this extension is attributed mainly to delayed end dates instead of the advanced beginning dates, and (3) the apparently delayed trends in end dates are associated with dominant regional cooling during late spring and summer months, while the insignificantly advanced trends in beginning dates correspond to inconsistent regional warming during late winter and spring months. On an interannual basis, growing season beginning and end dates correlate closely with mean air temperatures from February to April and from May to June, respectively. These findings imply that there are diverse seasonal response patterns by land vegetation to recent climate change in different parts of the world. Therefore, the results presented here provide new phenological evidence of climate change impacts from eastern Eurasia, and support the conclusion by the Intergovernmental Panel on Climate Change that climate change is already affecting living systems (McCarthy *et al*., 2001).

Further research may explore the possibility of temporal extrapolation of growing season parameters for years after 1993. In this way, we may carry out the spatial–temporal estimate of ground-based growing season at regional scales using plant phenology and satellite data.

Acknowledgements

The authors wish to thank Fuchun Zhang at CAS for providing the phenological data from 1989 to 1993 and Mark D. Schwartz at University of Wisconsin-Milwaukee for kindly revising the manuscript. Thanks to Weifeng Pan, Lin Ma, and Wenken Tan for processing phenology and satellite data. This research is funded by the National Natural Science Foundation of China under Grant No. 40371042.

References

Achard F, Blasco F (1990) Analysis of vegetation seasonal evolution and mapping of forest cover in West Africa with the use of NOAA AVHRR HRPT data. *Photogrammetric Engineering and Remote Sensing*, **56**, 1359–1365.

Ahas R (1999) Long-term phyto-, ornitho- and ichthyophenological time-series analyses in Estonia. *International Journal of Biometeorology*, **42**, 119–123.

Badeck FW, Bondeau A, Boettcher K *et al*. (2004) Responses of spring phenology to climate change. *New Phytologist*, **162**, 295–309.

Beaubien EG, Freeland HJ (2000) Spring phenology trends in Alberta, Canada: links to ocean temperature. *International Journal of Biometeorology*, **44**, 53–59.

Botta A, Viovy N, Ciais P *et al*. (2000) A global prognostic scheme of leaf onset using satellite data. *Global Change Biology*, **6**, 709–725.

Bradley NL, Leopold AC, Ross J *et al*. (1999) Phenological changes reflect climate change in Wisconsin. *Proceedings of National Academy of Sciences USA: Ecology*, **96**, 9701–9704.

Brandtner E (1958) *Methodische Untersuchungen an phaenologischen Beobachtungen unter besonderer Beruecksichtigung phytopathologischer Probleme*. Berichte des Deutschen Wetterdienstes Nr. 47, Offenbach, 14 pp.

Cannell MGR, Smith RI (1986) Climatic warming, spring budburst and frost damage on trees. *Journal of Applied Ecology*, **23**, 177–191.

Chen XQ (1994) *Untersuchung zur zeitlich-raeumlichen Aehnlichkeit von phaenologischen und klimatologischen Parametern in Westdeutschland und zum Einfluss geooekologischer Faktoren auf die phaenologische Entwicklung im Gebiet des Taunus*. Berichte des Deutschen Wetterdienstes Nr. 189, Offenbach, 116 pp.

Chen XQ (2003a) Assessing phenology at the biome level. In: *Phenology: An Integrative Environmental Science* (ed. Schwartz MD), pp. 285–300. Kluwer Academic Publishers, Dordrecht.

Chen XQ (2003b) East Asia. In: *Phenology: An Integrative Environmental Science* (ed. Schwartz MD), pp. 11–25. Kluwer Academic Publishers, Dordrecht.

Chen XQ, Pan WF (2002) Relationships among phenological growing season, time-integrated Normalized Difference Vegetation Index and climate forcing in the temperate region of Eastern China. *International Journal of Climatology*, **22**, 1781–1792.

Chen XQ, Tan ZJ, Schwartz MD *et al*. (2000) Determining the growing season of land vegetation on the basis of plant phenology and satellite data in Northern China. *International Journal of Biometeorology*, **44**, 97–101.

Chen XQ, Xu CX, Tan ZJ (2001) An analysis of relationships among plant community phenology and seasonal metrics of Normalized Difference Vegetation Index in the northern part of the monsoon region of China. *International Journal of Biometeorology*, **45**, 170–177.

Chmielewski FM, Roetzer T (2001) Response of tree phenology to climate change across Europe. *Agricultural and Forest Meteorology*, **108**, 101–112.

Chu CC (1964) Phenology and agricultural production. *New Construction*, **188–189**, 142–149 (in Chinese).

Chu CC, Wan MW (1973) *Phenology*. Science Press, Beijing (in Chinese).

Compilation Committee on the Vegetation of China (1980) *The Vegetation of China*. Science Press, Beijing (in Chinese).

Couvillon GA, Erez A (1985) Influence of prolonged exposure to chilling temperatures on bud break and heat requirement for bloom of several fruit species. *Journal of the American Society for Horticultural Science*, **110**, 47–50.

Duchemin B, Goubier J, Courrier G (1999) Monitoring phenological key stages and cycle duration of temperate deciduous forest ecosystems with NOAA/AVHRR data. *Remote Sensing of Environment*, **67**, 68–82.

Fisher A (1994) A model for the seasonal variations of vegetation indices in coarse resolution data and its inversion to extract crop parameters. *Remote Sensing of Environment*, **48**, 220–230.

Fitter AH, Fitter RSR (2002) Rapid changes in flowering time in British plants. *Science*, **296**, 1689–1691.

Gao YX, Xu SY, Guo QY, Zhang ML (1962) *Some Aspects on the Monsoon over East Asia*. Science Press, Beijing (in Chinese).

Goward SN, Markham B, Dye DG *et al*. (1991) Normalized difference vegetation index measurements from the advanced very high resolution radiometer. *Remote Sensing of Environment*, **35**, 257–277.

Haenninen H (1990) Modelling bud dormancy release in trees from cool and temperate regions. *Acta Forestalia Fennica*, **213**, 47.

Holben BN (1986) Characteristics of maximum-value composite images from temporal AVHRR data. *International Journal of Remote Sensing*, **7**, 1417–1434.

Hopkins AD, Murray MA (1933) Natural guides to the beginning, length and progress of the seasons. *Acta Phaenologica*, **2**, 33–43.

Institute of Geography at Chinese Academy of Sciences (1965) *Chinese Yearbook of Animal and Plant Phenological Observation No. 1*. Science Press, Beijing.

Institute of Geography at Chinese Academy of Sciences (1988) *Chinese Yearbook of Animal and Plant Phenological Observation No. 8*. Geology Press, Beijing.

Institute of Geography at Chinese Academy of Sciences (1989a) *Chinese Yearbook of Animal and Plant Phenological Observation No. 9*. Geology Press, Beijing.

Institute of Geography at Chinese Academy of Sciences (1989b) *Chinese Yearbook of Animal and Plant Phenological Observation No. 10*. Survey and Drawing Press, Beijing.

Institute of Geography at Chinese Academy of Sciences (1992) *Chinese Yearbook of Animal and Plant Phenological Observation No. 11*. Chinese Science and Technology Press, Beijing.

Justice CO, Townshend JRG, Holben BN *et al*. (1985) Analysis of the phenology of global vegetation using meteorological satellite data. *International Journal of Remote Sensing*, **6**, 1271–1318.

Keeling CD, Chin JFS, Whorf TP (1996) Increased activity of northern vegetation inferred from atmospheric CO_2 measurements. *Nature*, **382**, 146–149.

Kramer K (1996) *Phenology and growth of European trees in relation to climate change*. Thesis, Landbouw Universiteit Wageningen, 210 pp.

Lloyd D (1990) A phenological classification of terrestrial vegetation cover using shortwave vegetation index imagery. *International Journal of Remote Sensing*, **11**, 2269–2279.

Lucht W, Prentice IC, Myneni RB *et al*. (2002) Climatic control of the high-latitude vegetation greening trend and Pinatubo effect. *Science*, **296**, 1687–1689.

Malingreau JP (1986) Global vegetation dynamics: satellite observation over Asia. *International Journal of Remote Sensing*, **7**, 1121–1146.

Markon CJ, Fleming MD, Binnian EF (1995) Characteristics of vegetation phenology over the Alaskan landscape using AVHRR time-series data. *Polar Record*, **31**, 179–190.

McCarthy JJ, Canziani OF, Leary NA *et al* (eds) (2001) *Climate Change 2001: Impacts, Adaptations, and Vulnerability*. Cambridge University Press, Cambridge.

McMaster GS, Wilhelm WW (1997) Growing degree-days: one equation, two interpretations. *Agricultural and Forest Meteorology*, **87**, 291–300.

Menzel A (2003) Plant phenological anomalies in Germany and their relation to air temperature and NAO. *Climatic Change*, **57**, 243–263.

Menzel A, Fabian P (1999) Growing season extended in Europe. *Nature*, **397**, 659.

Moulin S, Kergoat L, Viovy N *et al*. (1997) Global-scale assessment of vegetation phenology using NOAA/AVHRR satellite measurements. *Journal of Climate*, **10**, 1154–1170.

Murray MB, Cannell MGR, Smith RI (1989) Date of budburst of fifteen tree species in Britain following climatic warming. *Journal of Applied Ecology*, **26**, 693–700.

Myneni RB, Keeling CD, Tucker CJ *et al*. (1997) Increased plant growth in the northern high latitudes from 1981 to 1991. *Nature*, **386**, 698–702.

Newman JE, Beard JB (1962) Phenological observations: the dependent variable in bioclimatic and agrometeorological studies. *Agronomy Journal*, **54**, 399–403.

Parmesan C, Yohe G (2003) A globally coherent fingerprint of climate change impacts across natural systems. *Nature*, **421**, 37–42.

Pfau R (1964) Varianz- und korrelationsanalytische Untersuchungen an phaenologischen Phasen im Naturraum 06 (Unterbayerisches Huegelland). *Meteorologische Rundschau*, **17**, 113–122.

Powell LE (1986) The chilling requirement in apple and its role in regulating time of flowering in spring in cold-winter climates. *Acta Horticulturae*, **179**, 129–139.

Powell LE, Swartz HJ, Pasternak G *et al*. (1986) Time of flowering in spring: its regulation in temperate zone woody plants. *Biologia Plantarum (PRAHA)*, **28**, 81–84.

Reed BC, Brown JF, VanderZee D *et al*. (1994) Measuring phenological variability from satellite imagery. *Journal of Vegetation Science*, **5**, 703–714.

Romberger JA (1963) *Meristems, growth and development in woody plants*. USDA Technical Bulletin, Nr. 1292, US Government Printing Office, 214 pp.

Root TL, Price JT, Hall KR *et al*. (2003) Fingerprints of global warming on wild animals and plants. *Nature*, **421**, 57–60.

Schnelle F (1955) *Pflanzen-Phaenologie*. Akademische Verlagsgesellschaft Geest & Portig K.-G, Leipzig.

Schwartz MD (1998) Green-wave phenology. *Nature*, **394**, 839–840.

Schwartz MD, Chen XQ (2002) Examining the onset of spring in China. *Climate Research*, **21**, 157–164.

Schwartz MD, Reed BC, White MA (2002) Assessing satellite-derived start-of-season measures in the conterminous USA. *International Journal of Climatology*, **22**, 1793–1805.

Schwartz MD, Reiter BE (2000) Changes in North American spring. *International Journal of Climatology*, **20**, 929–932.

Sparks TH, Jeffree EP, Jeffree CE (2000) An examination of the relationship between flowering times and temperature at the national scale using long-term phenological records from the UK. *International Journal of Biometeorology*, **44**, 82–87.

Viovy N, Arino O, Belward AS (1992) The best index slope extraction (BISE): a method for reducing noise in NDVI time-series. *International Journal of Remote Sensing*, **13**, 1585–1590.

Viovy N, Saint G (1994) Hidden Markov models applied to vegetation dynamics analysis using satellite remote sensing. *IEEE Transactions on Geoscience and Remote Sensing*, **32**, 906–917.

Walther GR, Post E, Convey P *et al* . (2002) Ecological responses to recent climate change. *Nature*, **416**, 389–395.

Wang JXL, Gaffen DJ (2001) Late-twentieth-century climatology and trends of surface humidity and temperature in China. *Journal of Climate*, **14**, 2833–2845.

White MA, Thornton PE, Running SW (1997) A continental phenology model for monitoring vegetation responses to interannual climatic variability. *Global Biogeochemical Cycles*, **11**, 217–234.

Worrall J (1998) Autumn leaf coloration. *Forest Chronology*, **74**, 668–669.

Worrall J (1999) Phenology and the changing seasons. *Nature*, **399**, 101.

Yang GD, Chen XQ (1995) *Phenological Calendars and their Applications in the Beijing Area*. Capital Normal University Press, Beijing (in Chinese).

Zhang JC, Lin ZG (1985) *The Climate of China*. Shanghai Science and Technology Publishers, Shanghai (in Chinese).

Zhang XY, Friedl MA, Schaaf CB *et al*. (2004) Climate controls on vegetation phenological patterns in northern mid- and high latitudes inferred from MODIS data. *Global Change Biology*, **10**, 1133–1145.

Zhou L, Tucker CJ, Kaufmann RK *et al*. (2001) Variations in northern vegetation activity inferred from satellite data of vegetation index during 1981 to 1999. *Journal of Geophysical Research–Atmospheres*, **106**, 20069–20083.